

Lateral Performance of a Temporary Bamboo Structure: Design and Experimental Assessment

J. Alami¹, M. A. Afshar^{2*}, A. A. Mazloun³

Received: 27 July 2021/Accepted: 12 November 2021
©KFRI (2021)

Abstract: Due to the disadvantages of using modern materials (e.g., steel and concrete), including unconventional extractions, exorbitant construction and production costs, and irreparable environmental damages, most countries have recently shifted towards the use of renewable and biodegradable natural resources to meet their needs. One of these resources is the bamboo plant. The aim of this study was to investigate the mechanical properties of a special bamboo species with the local name *Kara* (in Iran) and the typological name of *Bambusa pervariabilis*, and also performed modeling, analysis, and design of a temporary green structure of this plant against most of the loads prescribed by international codes. The Chevron brace was used as a lateral bearing element and hose-clamp connections were also employed. The results of compression, tensile, shear, shear with hose-clamp, and bending test parallel to the fibers were calculated to be 66.5, 103.42, 2.63, 2.73, and 137.96 MPa, respectively. The results of the analysis and design of the constructed model also indicated that the calculated demand under all load combinations in the elements of columns, beams, and braces for bending and axial stresses was more than 97%, and for shear stresses was more than 57% lower than the allowable capacity of the regulations.

Keywords: Analyzing, bamboo plant, green structure, mechanical properties, modeling.

*Corresponding Author

¹Graduated Master in structural Engineering,
Tarbiat Modares University, Tehran
E-mail: jalalalami21@yahoo.com

²Assistant Professor, Structural Engineering,
Imam Khomeini International University, Qazvin;
E-mail: mafshar@eng.ikiu.ac.ir

³Graduated Master in structural Engineering,
Imam Khomeini International University, Qazvin;
E-mail: AAmazloun@gmail.com

Introduction

The costs of production and construction of concrete and steel structures are heavy, and the interaction of these materials with bed soil causes a gray footprint in the site. The leachate of concrete, which penetrates into the bed soil, will not only damage the surrounding environment, but also pollutes the groundwater in some cases. Moreover, the energy required to produce 1 m³ of materials commonly used in construction, such as steel, is 50 times higher than the production of the same amount of bamboo (Azadeh, 2018). In recent decades, many researchers worldwide have argued that the use of the giant, fast-growing bamboo plant can adequately meet this requirement; by following a set of performance criteria, it can be a good alternative to very expensive and energy-wasting materials, such as steel and concrete (Lugt *et al.*, 2003). According to some sources in Iran, two places seem to be suitable for cultivating this plant: the northern strip of the country and a part of Khuzestan Province, located in the southwest (Azadeh, 2018). Bamboo is a composite material consisting of parallel cellulose fibers in a longitudinal direction placed in a wooden body (matrix). The density of fibers in the cross-sectional area of a bamboo shell varies along its thickness. These fibers are densely distributed in the outer surface area, and their dispersion in the inner cross-section is less than the outer cross-section (Liese, 1992; Ghavami, 2005). In essence, bamboo is a functional graded material that has evolved according to the state of stress distribution in its natural environment (Amada *et al.*, 1997; Amada and Untao, 2001; Nogota and Takahashi, 2005). The physical and mechanical properties of

bamboo are highly dependent on its fibers (Li *et al.*, 1995). The mechanical behavior of bamboo is non-isotropic and is very strong in the axial direction and weak in fiber plates (Moran *et al.*, 2017; Laura *et al.*, 2015). Based on the weight-to-weight ratio, very good comparisons are made between tensile strength, Young's modulus, compression strength, and shear between bamboo layers with conventional materials such as low-carbon steel and fiberglass-reinforced plastic (Ashby, 1992; Wegst *et al.*, 1993; Lakkad and Patel, 1981). Due to superior features and other factors such as low cost, easy access and lack of environmental damage caused by services, bamboo is widely used in the manufacturing industry (Lugt *et al.*, 2006; Chung and Yu, 2002; Chung and Chan, 2005; Yao and Li, 2003). Bamboo also is an eco-friendly and renewable plant (Janssen, 2000; Minke, 2012; Lugt *et al.*, 2005). Using of bamboo in the construction industry is still very limited due to the lack of appropriate regulations and design standards (Gat6o *et al.*, 2014) as well as the lack of a practical and reliable connection systems. To overcome these limitations, the use of steel hose-clamps in three different types of connections (bolted connections, steel hose-clamps only and hose-clamps and grouted infill mortar) was investigated. The purpose of this study was to calculate the rupture mode, load carrying capacity and ductility of bamboo joints and also to calculate the distance between the end length of the culm and the hose-clamp to obtain the optimal load carrying capacity and ductility. The results showed that, adequate length of the joints has led to significant gains in strength and ductility.

The results also mentioned that filling the joint with mortar leads to higher strength, but often at the cost of reducing ductility, compared to the relevant hollow joints with steel hose-clamps (Paraskeva *et al.*, 2019). Indonesia has faced many problems in the field of educational infrastructure for many years, in 2011 the country's building designers proposed a cheap, fast and sustainable solution to overcome this problem, bamboo. The results of building bamboo schools show undeniable savings in construction costs (Taufani *et al.*, 2014). However, bamboo is not yet recognized as a valuable material. Residential, governmental or institutional structures do not use bamboo, and the public perception is negative or neutral (Tenorio and Junior, 2003).

Materials and Methods

First, based on the research objectives, the studied bamboo and its curing methods are introduced. Then, according to the research process, the mechanical properties of the desired bamboo (compression, shear, tensile, and bending properties) are investigated. Next, modelling a temporary green structure in the OpenSees software. Finally, the analysis of software outputs are discussed.

Introduction of the Studied Bamboo

The studied bamboo is locally known as *Kara* (in Iran). This bamboo was named by the people of Gilan (a northern province of Iran) based on its appearance, geometry, method of growth, and use. Its scientific and typological name is *Phyllostachys*



Fig 1. Physical curing; (a) horizontal; (b) vertical position

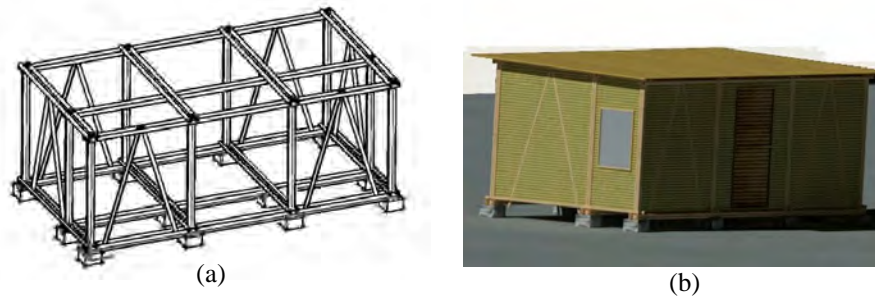


Fig 2. A 3D conceptual design of the proposed structure; (a) structural system; (b) structural views

vivax. This plant has an average outer diameter of 50 mm and an inner diameter of 38 mm. However, information on suitable growing conditions and water requirements is not available.

Treatment Methods

Bamboo curing is divided into three distinct types: (1) physical curing, (2) thermal curing, and (3) chemical curing. The first method was used in this paper. In the physical (traditional) process, which has long been common in East Asian countries, after cutting, the bamboo culms are placed vertically or horizontally (There are more recommendations for placement in the vertical direction) for 6-12 weeks in a place away from direct sunlight and with good ventilation. It is better to connect the bamboos to each other by wire or similar materials to prevent deformation and slipping of the culms (Fig. 1).

Analytical Experimental Estimates

A temporary green bamboo structure is modelled in OpenSees. A schematic three-dimensional (3D) view of this structure is displayed in Fig. 2. The proposed structure is located in the city of Kerman. This city

was chosen as it has experienced many earthquakes. For the design of this structure, IBC (International Building Code, 2018), Columbia NSR-10 (Resistant, Colombian Earthquake Construction Regulations, 2010) and the English translation of the Columbia Code, Unconventional and Indigenous Building Materials (Kent and Sharma, 2019), were used.

Method of Experimental Tests

Compression, shear, tensile, and bending tests were performed on the bamboo in accordance with ISO 22157 (International Standard ISO 22157-1: (E), 2019). The universal apparatus employed to perform the above tests was a Zwick Roell model with a capacity of 50 KN. For the bending test, a 60-ton semi-automatic concrete beam bending jack was used.

Analysis of Experimental Results

According to the regulations, specimens that have unreasonable results should be removed from the test results. Furthermore, according to ISO 22157 (2019), the number of specimens in each test should not be less than three. However, due to the lack of

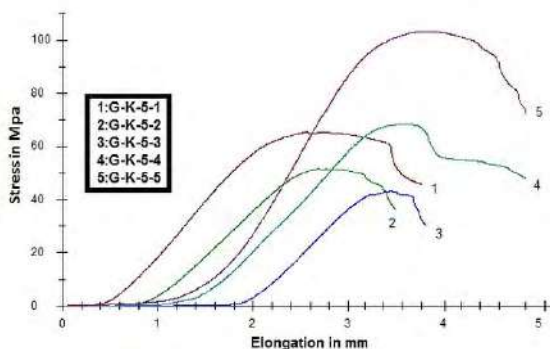


Fig 3. The compression test; (a) results; (b) specimens of Kara bamboo

adequate data from the cutting and type of division of each bamboo culm in the farm, it is impossible to accurately pinpoint the exact beginning and end of the culms. Therefore, the criterion for the top and bottom of each bamboo culm is a bamboo with a length of 2.5 m.

1. Compression Strength Test Parallel to the Fibers

The length of the specimen is taken as the lesser of the outer diameter, D , or 10 times the wall thickness, 10δ . Accordingly, the length of the specimens was considered equal to the outer diameter $L = 1D$. To set the center of the moving head of the machine vertically above the center of the cross-section of the specimen, an approximate initial load of 0.1 KN was applied to the specimen. Additionally, the load at a constant velocity of 0.1 mm/s was applied, and the maximum final load was recorded when the specimen failed (Jianchao *et al.*, 2016).

According to Fig. 3(a), the number of specimens was five, named G-K-1 to G-K-5. These specimens contain internal nodes and are selected sparsely from different heights of culms with different heights

of 2.5 m. Moreover, based on Fig. 3(a), it can be declared that the range of compression strength was between 50 and 60 in terms of MPa. This type of bamboo had an average compression strength of 66.5 MPa. Furthermore, although the maximum compression strength was 103.39 MPa for the G-K-5 specimen, the minimum was 43.31 MPa for the G-K-3 specimen. In addition, the reason why the amount of elongation and bearing capacity in specimens G-K-1, G-K-2 and G-K-3 is a small value is due to sudden rupture at the node. This phenomenon can be seen at the end of the stress- elongation curve of all three diagrams. However, specimens G-K-4 and G-K-5 experience large elongation and greater ultimate strength due to both tensile failure along the transverse bamboo culm and Poisson properties and peripheral tensile strains.

The average modulus of the compression elasticity of the parallel axis of the fibers was equal to 2.03 GPa. The results obtained from the compression strength test parallel to the fibers and according to the existing geometric characteristics were consistent with the results of other tests with acceptable

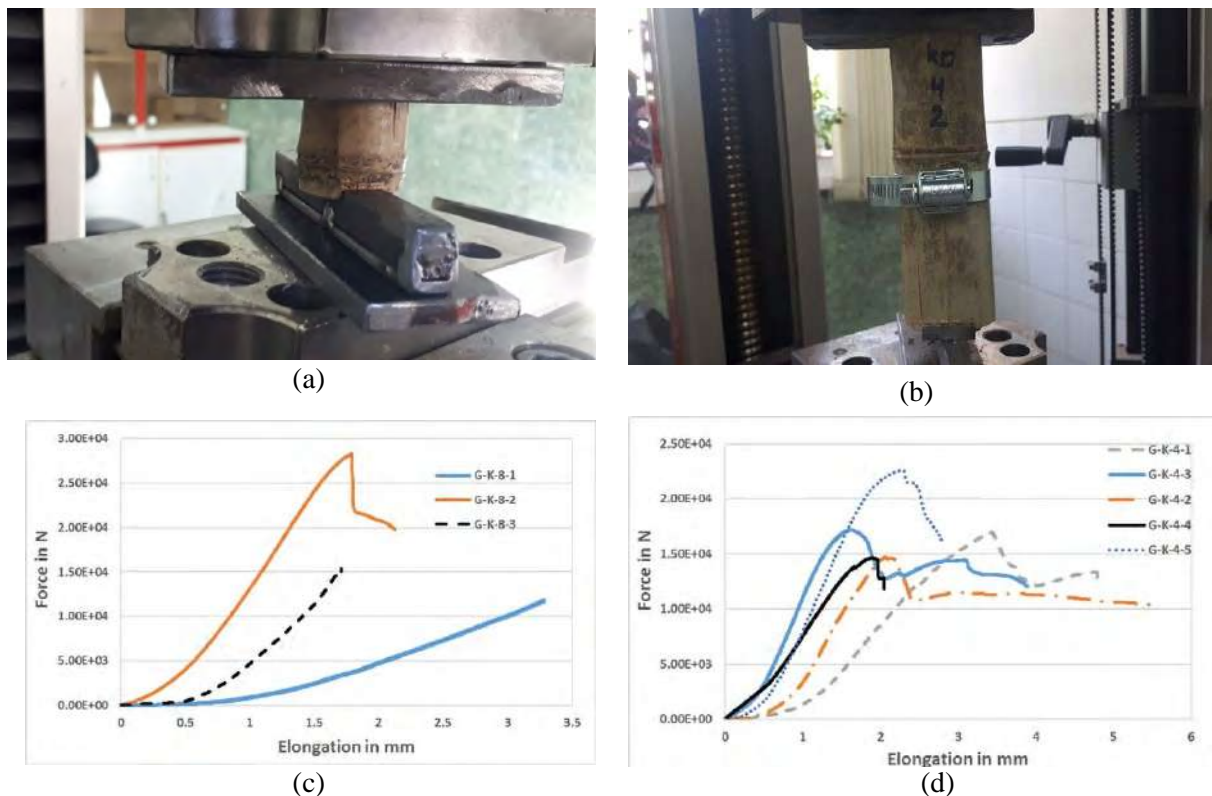


Fig 4. Shear test machine; (a) without a hose-clamp; (b) with a hose-clamp; shear test results; (c) without a hose-clamp; (d) with a hose-clamp

Table 1. Shear test results

Type	Specimen	Out-diameter	In-diameter	Fult (N)	Fv (Mpa)
Without hose-clamp	G-K-8-1	50	35	1.18E+04	1.68
	G-K-8-2	50	35	2.83E+04	4.04
	G-K-8-3	50	36	1.55E+04	2.16
With hose-clamp	G-K-4-1	43	31	1.72E+04	2.43
	G-K-4-2	42	31	1.47E+04	2.34
	G-K-4-3	41	31	1.72E+04	3.04
	G-K-4-4	41	31.5	1.46E+04	2.71
	G-K-4-5	41	27.5	2.26E+04	3.11

proportions (Perilaku, 2001). Fig. 3(b) presents an overview of the specimens after the experiment. It is clear that all the specimens were squeezed, deep cracks were created in the direction of the fiber, and the diaphragm zone of the node was broken.

Equations (P-1) and (P-2) in Appendix (A) were used to calculate the compression strength and the compression elasticity modulus parallel to the fibers.

2. Shear Strength Test Parallel to the Fibers

According to Subsection 13.1.2 of ISO 22157 regulation (2019), the specimen is supported at its lower end over two opposing quadrants, and loaded at its upper end over the other two opposing quadrants. In this manner, loading the specimen results in four shear areas. This test was conducted via two distinct methods, with a steel hose-clamp and without a hose-clamp. The purpose of examining the results of the specimens with steel hose-clamp was to investigate the rate of increase in the bamboo shear strength and the improvement in the performance of bamboo in the joints. In this test, the number of specimens whose results can be recorded is three in the case without the hose-clamp (G-K-8-1 to G-K-8-3) and five in the case with the hose-clamp (G-K-4-1 to G-K-4-5). Note that specimen naming is optional.

Figs. 4(a) and (b) depict how shear tests are performed. From Fig. 4(c), it can be observed that the first and third specimens (G-K-8-1 and G-K-8-3) were perfect examples of very brittle behavior (When the maximum shear force is applied to the specimen, the specimen experiences rupture immediately).

The second specimen (G-K-8-2) of the Kara bamboo had a softer behavior than the other two speci-

mens, and a little after the yield (about 1.6 mm), a rupture occurred in it (about 2.2 mm). In other words, behaviour the long length between the yield point and the rupture point indicates the appropriate ductile behavior of the specimen and vice versa, i.e. the shorter distance denoted, the more brittle behavior. The specific reason for kink for G-K-8-2 was due to a sudden decrease in local buckling at the location of the internal node. Based on Fig. 4(d), four out of the five specimens reached maximum shear force at a certain elongation range (< 2 mm). The first, second, third, and fifth specimens reached the rupture threshold point at an elongation of < 3 mm. The first specimen, as an exception, reached a maximum shear force in the elongation of about 2 times greater than that of the other specimens and experienced the rupture stage in a elongation of < 6 mm, respectively. From Table 1, in the case without a hose-clamp, the maximum shear strength of 4.04 MPa belonged to the second specimen, while the minimum value was 1.68 MPa for the first specimen.

Also, in the case of steel hose-clamps, the fifth specimen with a shear strength of 3.11 and the second specimen with 2.34 MPa resulted in the highest and lowest strength, respectively. The use of steel hose-clamps not only prevents the expansion of cracks, especially longitudinal cracks in the direction of the element, but also significantly increases the duration of operation of the element. Eq. (P-3) in Appendix (B) was used to calculate the shear strength parallel to the fibers.

3. Tensile Strength Test Parallel to the Fibers

Based on Subsection 11.2 of the ISO 22157 code (2019), at least three specimens must be extracted

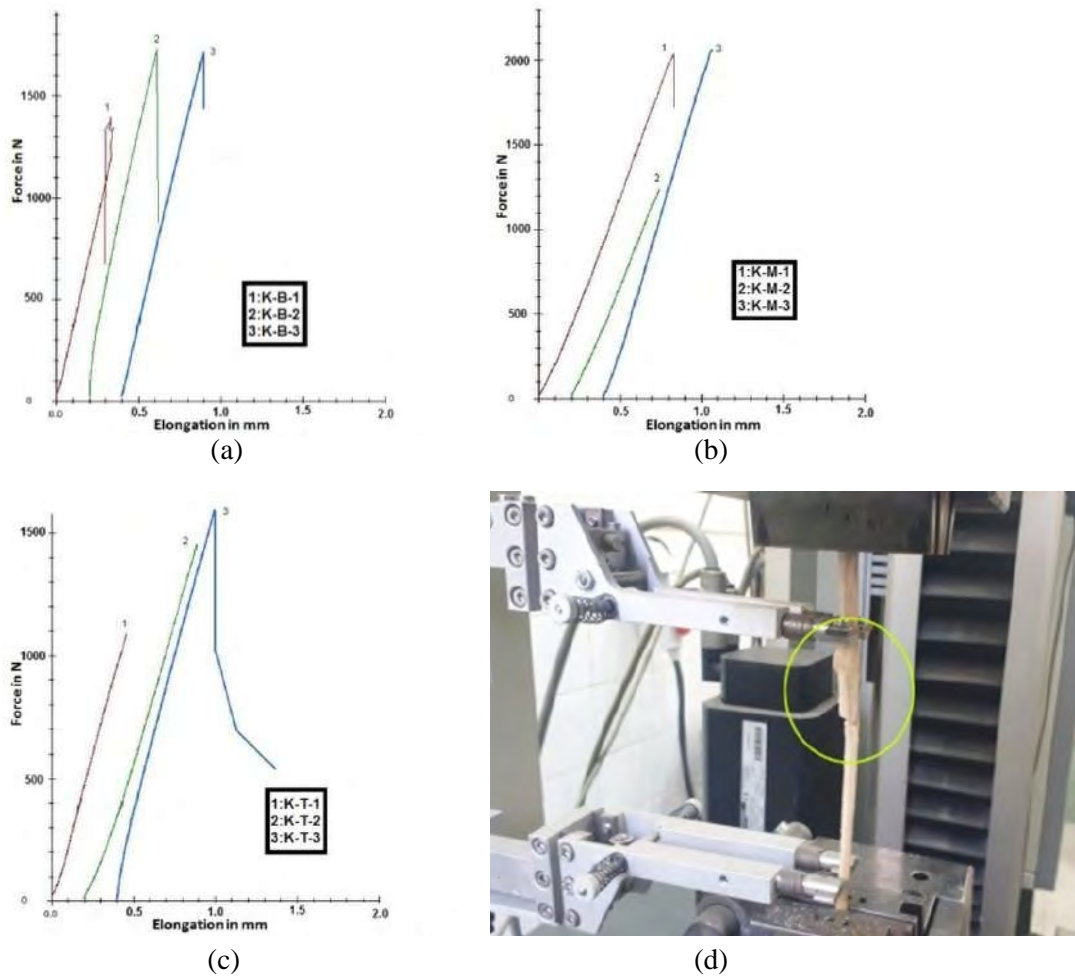


Fig 5. Results of Kara bamboo tensile test; (a) bottom part; (b) middle part; (c) top part of the culm; (d) the tensile test apparatus

from each bamboo culm in order to account for variability within the culm. Fig. 5(d) shows how the test was performed. Kara bamboo was examined as a complete culm, in which one culm was divided into three parts: upper, middle, and lower, and from each, three specimens were split and examined separately.

Fig. 5(a-c) presents a complete Kara bamboo culm. According to all three diagrams, it can be stated that by moving from the bottom of the culm to its top, the behaviors become more brittle (except for the third specimen in Fig. 5(c), which has shown the softest behavior against tensile failure). In Fig. 5(a) graph line 1 (K-B-1) shows that at the same force the elongation decreased. It seems, it is due to the strain gauge snap back on the verge of rupture.

According to Fig. 5(a-c), failure in all the specimens occurred in the areas close to the node, within the 100 mm area of the strain gauge arms (type gauge:

ETC-EXMACRO.001). It can also be inferred from Table 2 that the middle part of the culm experienced the highest strength and modulus of tensile elasticity (approximately 25% more than the lower and upper parts of the bamboo culm). It should be mentioned again that by a full culm, we refer to a culm with a length of 2.5 m which was available to the researchers; unfortunately, complete information about the full culm with a length of more than 10 m was not available. Equations (P-4) and (P-5) in Appendix (C) were used to calculate the tensile strength and the tensile elasticity modulus parallel to the fibers.

4. Bending Strength Test Parallel to the Fibers

According to Subsection 12.3 of ISO 22157 regulation (2019), to achieve bending failure, the distance between each support and the closest point to which the load is applied must be at least 10D, where D is

Table 2. Tensile test results

Type	Position	Num.node	Specimen	b (mm)	δ (mm)	F(t,0) (Mpa)	E(t,0) (Mpa)
	Bottom	1	K-B-1	3	5.2	89.51	2.31E+04
		1	K-B-2	3	5.3	108.79	2.46E+04
		1	K-B-3	3	5.1	111.98	2.27E+04
Kara	Middle	1	K-M-1	2.32	4.31	203.61	2.54E+04
		1	K-M-2	2.31	4.51	106.66	2.17E+04
		1	K-M-3	2.32	4.31	206	3.30E+04
	Top	1	K-T-1	2.12	4.31	119.79	2.80E+04
		1	K-T-2	2.31	4.52	139.24	2.09E+04
		1	K-T-3	2.24	4.31	165.11	2.65E+04

the outer diameter of the bamboo specimen. Both shear spans must be the same. The minimum distance between the loading points should be 10 D; therefore, the minimum culm length should be considered 30 D. The speed of the test based on the ISO standard should be such that it can satisfy the required time (300 ± 120 seconds). For more information, see Section (d) in the appendix. From Table 3, it can be concluded that the highest bending moment belonged to the second specimen with a value of $8.30E+5$ N.m, which was followed by the fifth, fourth, first, and third specimens, respectively. According to the values calculated for the tangent bending stiffness, it can be stated that all the specimens showed a soft behavior during loading. Furthermore, the mean bending moment and the tangent bending stiffness were calculated as $6.41E+5$ N.m and $2.42E+10$ N.m², respectively. The results obtained from the bending test parallel to the fibers were consistent with the results of other tests with acceptable proportions (Jagadish et al., 2010). Equations (P-6) to (P-8) in Appendix (D) were used for calculations in this section.

Modeling, Analysis, and Design

The plan of the proposed structure is displayed in Fig. 6(e). The structure had was 3 m wide, 6 m long, and 2.5 m high. Four types of columns in this plan were specified; the columns shown with C4 had a height of 0.2 m (from the ground level to the floor level), but the other columns had a height of 2.5 m. Type C1 columns were located around the structure and are called corner columns. Columns C2 and

C3 were the middle columns in the longitudinal and transverse directions, respectively. Moreover, type B1 beams were in the longitudinal direction, type B2 beams were in the transverse direction, and type B3 beams were the sub-beams in the plan. The braces in this plan were designed and modeled by the Chevron brace type. The arrangement of bamboo culm in the columns and beams is depicted in Figs. 6 (a-d). The way the beams are placed around the column is known as a satchel connection. Due to the little rainfall in the area, the roof of the structure was a low slope roof. The dead load and the live load of the floor were equal to 55.5kg/m and 200kg/m, respectively.

Furthermore, the dead load of the roof was 63.75kg/m, the live load of the roof was 150kg/m, the wall load was 91.87kg/m, and the snow load was 0.56KN/m². The wind load in KN is shown in Fig 7. Currently, there are no regulations or standards for the design of bamboo structures in the LRFD method (Kent and Sharma, 2019). Therefore, the method used for analysis and design in this paper was the allowable stress method (ASD). The loads' combination of allowed stress is presented in Table 4 (International Building Code, 2018). The Kara bamboo characteristics, calculated by the experiments, are presented in detail in Table 5. In the seismic analysis, investigated in the form of time history analysis, three earthquakes of Bam, Manjil, and Thebes were studied in two orthogonal directions. The examined earthquakes were scaled according to the Iranian code of practice

Table 3. Bending test results

Type	Position	L	a	I _b	M _{ult}	F _(m,0)	E _{(m,0),I_b}
Kara	K-1	1237.5	412.5	107404.9	5.57E+05	75.1799	1.59E+10
	K-2	1245	415	76058.45	8.30E+05	188.2434	1.51E+10
	K-3	1206	402	69982.13	5.43E+05	127.9548	3.74E+10
	K-4	1236	412	79612.74	6.18E+05	130.0232	3.72E+10
	K-5	1230.9	410.3	67700.71	6.56E+05	168.3849	1.53E+10

Units are in terms of Newton and millimeters.

for seismic resistant design of buildings (Iranian Code of Practice for Seismic Resistant Design of Buildings, 2014). In Fig. 8(a), the response spectrum of each pair of accelerograms is combined by using the Root-mean-square method (RMS); a single composite spectrum is made for each pair of accelerograms, and then the acceleration spectrum of all three earthquakes are shown. The RMS along with the standard design spectrum (type three soil) is shown in Fig. 8(b). Furthermore, the period of this proposed temporary structure is equal to T=0.064 seconds. According to Subsection 2-5-3 of Standard 2800 (2014), the mean value of the RMS should be scaled so that it does not fall below the line of the standard design spectrum in the time interval of 0.2T to 1.5T. The structure ductility coefficient (R) and the building priority factor (I) equaled 1.6 and 0.8, respectively (Resistant, Colombian Earthquake Construction Regulations, 2010) and (Kent and Sharma, 2019).

Regulation Design Criteria

According to G.12.10 of NSR-10 (Resistant, Colombian Earthquake Construction Regulations, 2010) and (Kent and Sharma, 2019), the following equations were used to control the bearing capacity of the elements: First, Eq. 1 was used to calculate the allowable stresses.

$$(F_i)' = F_i CD CM Ct Cl Cr Cc \tag{1}$$

Where, F_i is the stresses calculated from the experimental studies presented in Table 5. The adjustment factors belong to loading duration (CD), moisture content (Cm), temperature (Ct), beam lateral stability (CL), group action (Cr) and shear (Cc), the sum of the correction coefficients of this equation. These coefficients are aggregated in Table 14.3 of (Kent and Sharma, 2019) and Table 6 in this study. Table 6 shows the allowable stress values obtained from Eq. 1. In this table, (F_c)' is the allowable compress-

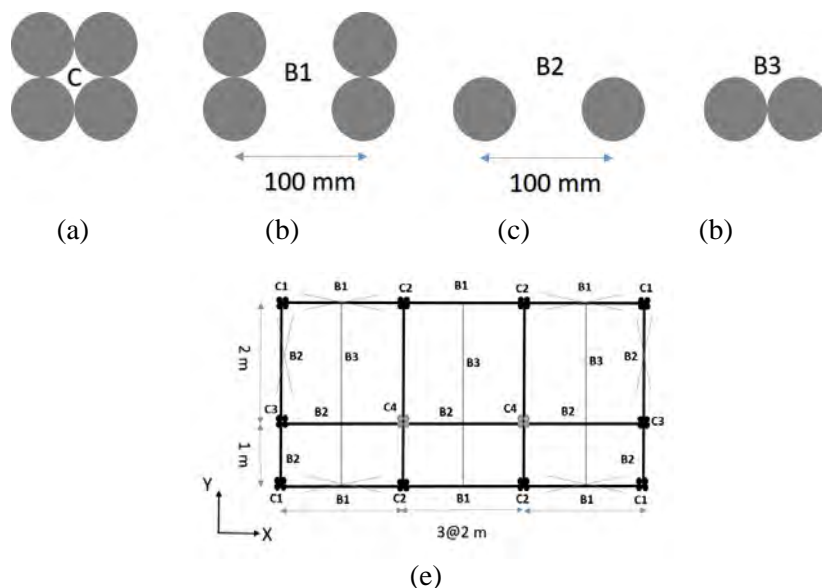


Fig 6. Arrangement of bamboo culms in (a) column; (b) beam with type B1; (c) beam with type B2; (d) beam with type B3; (e) structural plan

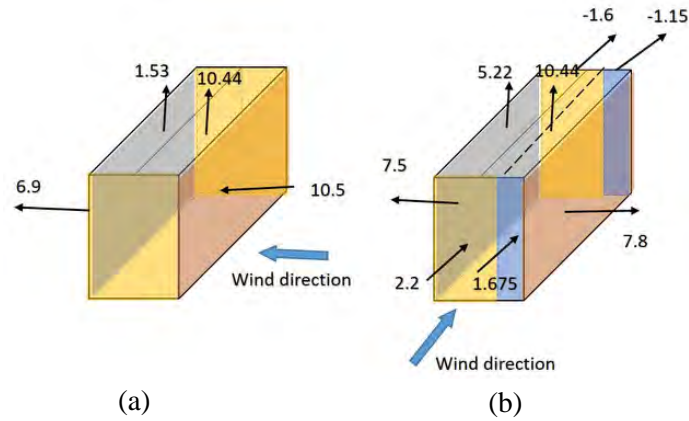


Fig 7. Schematic view, wind load distribution, and force intensity (KN); (a) north to south; (b) east to west

sion stress, $(F_b)'$ is the allowable bending stress, $(F_t)'$ is the allowable tensile stress, and $(F_v)'$ is the allowable shear stress. Then, Eqs. (2) and (3) were used to control the bearing capacity of the elements. Here, the combined effect of the internal stresses of each element should not be more than one.

$$f_t/(F_t)' + f_b/(F_b)' \leq 1 \quad (2)$$

$$f_c/(F_c)' + (k_m f_b)/(F_b)' \leq 1 \quad (3)$$

In Eq. 2, f_t and f_b denote the acting tension and bending stresses over the element, respectively. Similarly, in Eq. 3, f_c corresponds to the acting compression stresses over the element. Also, for the bending moment occurring simultaneously with the compression force, second-order bending stress, known as the P- Δ effect, is induced. In order to account for this effect, the actual bending stress is multiplied by an amplification factor, k_m given, by Eq. 4. Additionally, N_a is the acting compression force, and N_{cr} is Euler critical buckling load

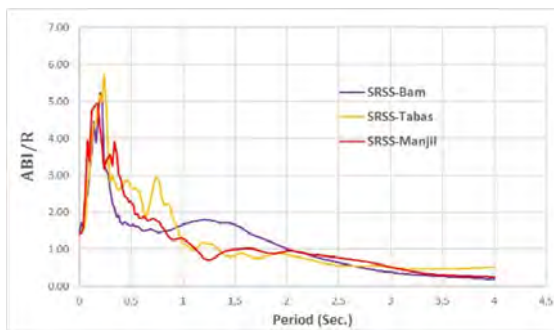
calculated using the fifth percentile modulus of elasticity, $E_{0.05}$.

$$k_m = 1/(1 - 1.5(N_a/N_{cr})), N_{cr} = (\pi^2 E_{0.05} I)/(k_l^2) \quad (4)$$

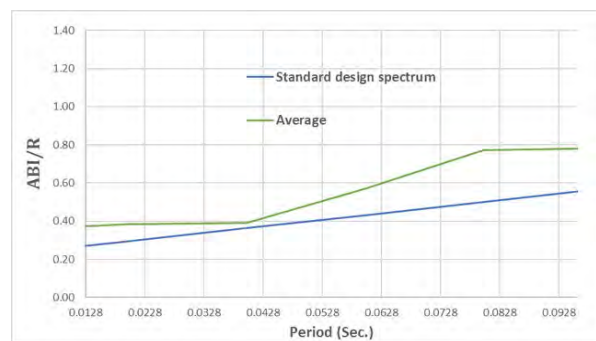
The values of $E_{0.05}$ and E_{min} are calculated from the following equation: In Eq. 5, which is consistent with the Colombian Code NSR-10 (Section G.A.1) (2017), the value of covariance was considered equal to 0.16.

$$E_{0.05} = E(1 - 1.645COV_E), E_{min} = 1.03E_{0.05/1.66} \quad (5)$$

To evaluate the experimental results, a very powerful software (OpenSees) was utilized. The sample considered in software modeling was a single column with two nodes. The length of the sample was 200 mm, the outer diameter was 47.6 mm, and the inner diameter was 37.1 mm. All units of measurement were introduced to the software in newton, meter, and second. The materials' information introduced to the program was in accordance with Table 5.



(a)



(b)

Fig 8. Earthquake spectrum; (a) the square sum root of the three earthquakes; (b) the comparison of the soil spectrum and the mean spectrum

Table 4. Loads' combination (ASD)

Combination	Equation	Combination	Equation
Comb1	DL	Comb11	DL+0.45We+0.75LL+0.75Lr
Comb2	DL+LL	Comb12	DL+0.45We+0.75LL+0.75S
Comb3	DL+Lr	Comb13	DL+0.45Wn+0.75LL+0.75Lr
Comb4	DL+S	Comb14	DL+0.45Wn+0.75LL+0.75S
Comb5	DL+0.75LL+0.75Lr	Comb15	DL+0.525Ex+0.75LL+0.75S
Comb6	DL+0.75LL+0.75S	Comb16	DL+0.525Ey+0.75LL+0.75S
Comb7	DL+0.6We	Comb17	0.6DL+0.6We
Comb8	DL+0.6Wn	Comb18	0.6DL+0.6Wn
Comb9	DL+0.7Ex	Comb19	0.6DL+0.7Ex
Comb10	DL+0.7Ey	Comb20	0.6DL+0.7Ey

First, to introduce the stress-strain curve in the compression and tensile part, the rate of change in the length obtained from the experimental results became non-dimensional (converted to strain) and, then, the mean strain of all the specimens was taken. Next, all the forces obtained from both the experimental compression and tensile tests were converted into stresses, and finally, the average stresses were calculated and plotted (see Fig. 9). In OpenSees, this stress-strain curve was introduced by multi-linear elastic materials (UniaxialMaterial ElasticMulti-Linear). The fiber code (Section Fiber) was used to model the cross-section, and the non-linear element code of beams and columns was employed to introduce the element (Element nonlinearBeamColumn).

In order to model the steel hose-clamps in the areas close to the connections, several nodes were created, and then the relevant specifications were utilized to model the elements of those areas according to

Table 6. From Fig. 9, it can be concluded that the results of software had a very small percentage of error (about 0.001) compared to the experimental results; in other words, the software results were very similar to the experimental results. G-K-5-1 to G-K-5-5 were the specimens of bamboo used in this compression test, and K-T-1, K-T-2, and K-T-3 were the specimens used in the tensile test. Specimen naming is optional.

Modeling Results

In Eqs. (2) and (3), all the results of the maximum ratio of demand to the load-bearing capacity of the elements must be < 1 . Now, based on the results of controlling the capacity of the elements presented in Table 7, it is clear that all the results were much smaller than the value of 1 and, accordingly, the elements' responses were very desirable. For example, for columns, the demand amount for

Table 5. Mechanical characteristics of Kara bamboo

Type	Values
Mass	0.584 Kg
Compression strength	66.5 MPa
Bending strength	137.96 MPa
Tensile strength	103.42 MPa
Shear strength	2.63 MPa
Shear strength with Hose-clamp	2.72 MPa
Modulus of elasticity	23482 MPa

Table 6. Correction coefficients and allowable stresses

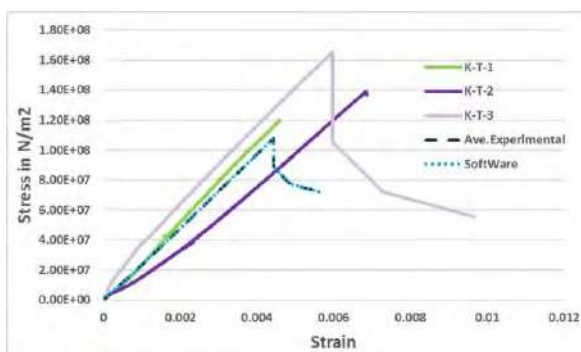
		E_{min}	$E_{0.05}$	E	f_v	f_c	f_t	f_b
C_D	Ten years	1				1	1	1
C_M	0.15%	0.87	0.96	0.96	0.96	0.91	0.87	0.91
C_t	$T \leq 37'$	1	1	1	1	1	1	1
C_l	Beam/column	1	-	-	-	-	-	-
C_r	-	1	-	-	-	1	1	1
C_c	-	-	-	-	0.93	-	-	-
Allowable stresses (MPa)		$(F_v)'$	$(F_c)'$	$(F_t)'$	$(F_b)'$			
		2.4	57.9	94.1	120			

element capacity was estimated to be 97.2% more favorable than the allowable limit of the regulations. Table 7 also presents the load combination of the maximum demand-to-capacity ratio per element. According to the combination of the introduced loads as well as the recommendations of codes for temporary structures, it can be observed that the wind load to this structure prevailed over the seismic load.

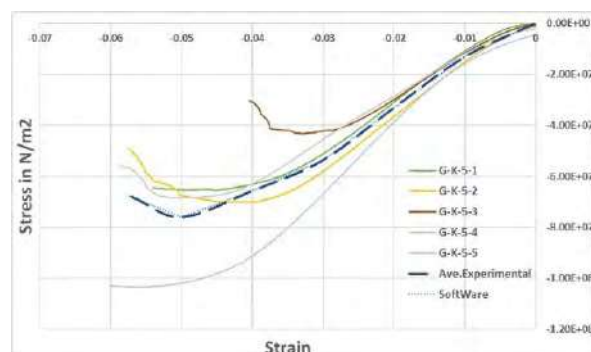
Special attention should be paid to the fact that bamboo stems are very weak against shear stresses. In Subsection G.12.8.11.2 of NSR-10 (2017), the ratio of maximum shear stresses applied to the element to the allowable shear stress should not exceed 1. Hence, this issue was also examined in Table 7, and the results indicated the appropriate resistance of the elements against shear stresses. To

achieve better shear stress resistance, especially at the joints, steel hose-clamps are used in the areas close to the joints. As mentioned before, the use of steel hose-clamp not only prevents the expansion of cracks, especially cracks occurring in the longitudinal direction of the element, but also leads to a dramatic growth of the operating time of the structure. Table 7 presents the columns related to the ratio of shear stresses with hose-clamps and without hose-clamps. It is obvious that the stress ratio response in the case with steel hose-clamps was about 3.4% more appropriate than the case of connections without using these clamps.

The examination of construction costs is essential to proposing and designing new structures. However,



(a)



(b)

Fig 9. Results from validation; (a) tensile; (b) compression point

Table 7. Modeling output results

Element	Type	Length (m)	Demand to capacity ratio	Combination	Shear stress ratio	Shear stress ratio with hose-clamp
Column	C1	2.5	0.028	Comb8	0.4261	0.4115
Column	C2	2.5	0.028	Comb8	0.4261	0.4115
Column	C3	2.5	0.028	Comb8	0.4261	0.4115
Beam	B1	1	2.94E-6	Comb18	0.2631	0.2541
Beam	B2	2	4.71E-4	Comb12	0.4412	0.4262
Brace	X-direction	2.47	0.016	Comb18	-	-
Brace	Y-direction	2.47	0.09	Comb15	-	-

since there is no specific source for this evaluation, the experiences and knowledge of the constructors were used for this purpose. Table 8 provides a general comparison of the estimated costs of constructing a temporary structure such as a residential CONEX box with dimensions equal to those of the proposed structure. The price per square meter in USD for different types of temporary structures was examined. Temporary structures made of siding sheet and sandwich panels were among the most expensive categories available (priced at > \$ 3,000 for a temporary structure with dimensions of 18 m²).

The cheapest steel structure for temporary structures was made of iron profiles which are not very popular due to the method and model of construction and the quality of materials. The proposed temporary green structure with a price per square meter of 30-35 USD seems a very reasonable option (The

mentioned prices are based on the prices available in Iran). Due to the use of plant materials, this temporary structure is preferable to others in terms of aesthetics, environmental friendliness, biodegradability, and much lower costs (about 60% compared to iron profiles, and 80% to sandwich panels) of design and construction.

In Iran, like other countries, bamboo has the same shear, tensile, compression, and bending strengths in relation to the same external diameter, according to the experimental results. Based on the results of tests performed on the specimens, *Kara* bamboo has a compression strength of 66.5 MPa, which is 160% more than conventional concrete (C25). Also, the tensile, bending, shear, and shear strengths with steel hose-clamp of the *Kara* bamboo are equal to 103.42, 137.96, 2.63, and 2.72 MPa, respectively. Nevertheless, the tensile strength of bamboo is

Table 8. Prices of the temporary structure (in Iran)

Type	Material	Length (m)	Width (m)	Price per m ² (\$)	Total Price (\$)
	Iron sheet profiles	6	3	75-84	1350-1500
	Sandwich panel	6	3	154-167	2775-3000
	Siding sheet	6	3	167-179	3000-3225
Temporary	Siding and galvanizing	6	3	133-146	2400-2625
	Galvanized sheet	6	3	92-104	1650-1875
	Bamboo	6	3	30-35	540-615

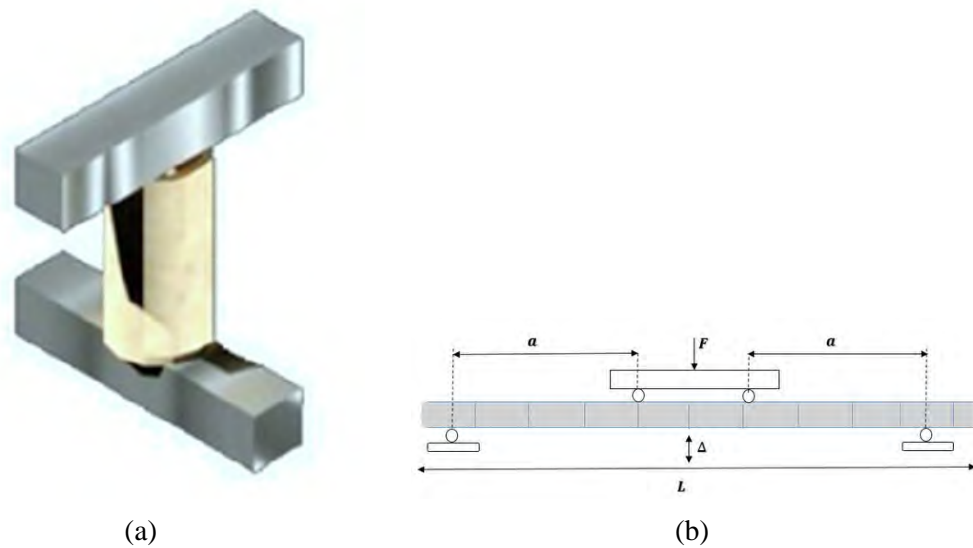


Fig 10. Schematic view of (a) shear test; (b) bending test apparatus

estimated to be approximately 50% lower than that of ST-37 steel.

The cost of building a temporary green bamboo structure is estimated to be about 60% more economical than a steel sample (Taufani *et al.*, 2014) and (information from field assessments).

The analysis of the modeling results of a bamboo structure also revealed that the demand-to-capacity ratio in columns and beams was 97.2% and 99.95% lower than the allowable limit of the Colombian Code, respectively. Furthermore, in the case of shear stresses, the stresses of the columns and beams were 57.39% and 64.78% more desirable than the allowable limits of the regulations, respectively.

Based on the results obtained from the structural analysis with the software as well as the experimental tests, the use of steel hose-clamps, especially in areas close to the joints, enhances the shear strength of the element by 3.4%. Preventing the expansion of crack length and depth and dramatically increasing the duration of operation of the element are the benefits of using steel hose-clamps in the joint areas. Accordingly, their application is highly recommended.

By using hose-clamps in the joints of the proposed structure, the safety margin of the joint against the dominant rupture mode, which is common in shear joints, is improved.

In the proposed temporary green structure, due to the low importance of the structure, the small number of floors (one floor), and a very low demand ratio due to the combination of loads to the allowable capacity of regulations, the use of recyclable, eco-friendly, and inexpensive materials such as bamboo are preferred to expensive materials such as concrete and steel that pose a serious threat to nature.

Author Contributions: M.A.Afshar: Conceptualization, software, supervision, and project administration. J.Alami: methodology, analysis, validation, writing—review and editing, and project administration. A.A.Mazloum: Conceptualization, software, validation, analysis, investigation, and visualization.

This research did not receive any specific grant from funding agencies in the public, commercial, or not-for-profit sectors.

Acknowledgments

Sincere thanks to the laboratory expert of Imam Khomeini International University, Ms. Chadorbaf.

Also appreciation for the tireless and countless efforts of Dr. Simiari.

References

- Azadeh, A. 2018. *Dendrocalamus Giganteus* Bamboo (Doctoral dissertation, PUC-Rio)
- Van Der Lugt, P., Van den Dobbelsteen, A. A. J. F. Abrahams, R. 2003. Bamboo as a building material alternative for Western Europe? A study of the environmental performance, costs and bottlenecks of the use of bamboo (products) in Western Europe. *Journal of Bamboo and Rattan*, 2(3), 205-223.
- Liese, W. 1992. The structure of bamboo in relation to its properties and utilization. In Zhu, S., Li, W., Zhang, X. Wang, Z. ed., *Bamboo and its use. Proceedings of the International symposium on Industrial Use of Bamboo*, Beijing, China pp. 7-11
- Ghavami, K. 2005. Bamboo as reinforcement in structural concrete elements. *Cement and concrete composites*, 27(6), 637-649.
- Nogata, F, Takahashi, H. 1995. Intelligent functionally graded material: bamboo. *Composites Engineering*, 5(7), 743-751.
- Amada, S., Ichikawa, Y., Munekata, T., Nagase, Y. Shimizu, H. 1997. Fiber texture and mechanical graded structure of bamboo. *Composites Part B: Engineering*, 28(1-2), 13-20.
- Amada, S, Untao, S. 2001. Fracture properties of bamboo. *Composites Part B: Engineering*, 32(5), 451-459.
- Li, S. H., Zeng, Q. Y., Xiao, Y. L., Fu, S. Y. Zhou, B. L. 1995. Biomimicry of bamboo bast fiber with engineering composite materials. *Materials Science and Engineering: C*, 3(2), 125-130.
- Moran, R., Webb, K., Harries, K. García, J. J. 2017. Edge bearing tests to assess the influence of radial gradation on the transverse behavior of bamboo. *Construction and Building Materials*, 131, 574-584.
- Villegas, L., Morán, R. García, J. J. 2015. A new joint to assemble light structures of bamboo slats. *Construction and Building Materials*, 98, 61-68.
- Ashby, M. F. Cebon, D. 1993. Materials selection in mechanical design. *Le Journal de Physique IV*, 3(C7), C7-1.
- Wegst, U. G. K., Shercliff, H. R. Ashby, M. F. 1993. The structure and properties of bamboo as an engineering material.
- Lakkad, S. C. Patel, J. M. 1981. Mechanical properties of bamboo, a natural composite. *Fibre science and technology*, 14(4), 319-322.
- Van der Lugt, P., Van den Dobbelsteen, A. A. J. F, Janssen, J. J. A. 2006. An environmental, economic and practical assessment of bamboo as a building material for supporting structures. *Construction and building materials*, 20(9), 648-656.
- Chung, K. F, Yu, W. K. 2002. Mechanical properties of structural bamboo for bamboo scaffoldings. *Engineering structures*, 24(4), 429-442
- Yu, W. K., Chung, K. F., & Chan, S. L. (2005). Axial buckling of bamboo columns in bamboo scaffolds. *Engineering Structures*, 27(1), 61-73.
- Yao, W, Li, Z. 2003. Flexural behavior of bamboo-fiber-reinforced mortar laminates. *Cement and concrete research*, 33(1), 15-19.
- Janssen, J. J. 2000. Designing and building with bamboo (pp. 130-133). Netherlands: International Network for Bamboo and Rattan
- Minke, G. 2012. *Building with bamboo: design and technology of a sustainable architecture*. Walter de Gruyter.
- Van der Lugt, P., Van den Dobbelsteen, A. A. J. F, Janssen, J. J. A. 2006. An environmental, economic and practical assessment of bamboo as a building material for supporting structures. *Construction and building materials*, 20(9), 648-656.
- Gatóo, A., Sharma, B., Bock, M., Mulligan, H. Ramage, M. H. (2014, October). Sustainable structures: bamboo standards and building codes. In *Proceedings of the Institution of Civil Engineers-Engineering Sustainability* (Vol. 167, No. 5, pp. 189-196). Thomas Telford Ltd.
- Paraskeva, T., Pradhan, N. P., Stoura, C. D. Dimitrakopoulos, E. G. 2019. Monotonic loading testing and characterization of new multi-full-culm bamboo to steel connections. *Construction and Building Materials*, 201, 473-483.

- Taufani, A. R., & Nugroho, A. S. B. (2014). Proposed bamboo school buildings for elementary schools in Indonesia. *Procedia Engineering*, 95, 5-14.
- Tenorio, R, Junior, J. D. C. 2020. Fomenting the Bamboo Building industry in Timor-Leste: Changing public perception, enhancing research and land governance with social partnerships. *Journal of Bamboo and Rattan*, 19(1), 1-12.
- Jagadish, V., Shruthi, R. Raghunath, S. 2010. Strength and elastic properties of bamboo elements used for housing. *Journal of Bamboo and Rattan*, 9(1/2), 29-47
- Kelechava, B. 2018 . International Building Code (ICC IBC-2018),”. American National Standards Institute Blog, available at< <https://blog.ansi.org/2017/11/2018-international-building-code-icc-ibc/#gref>>(last visited March 20, 2019). Google Scholar.
- Colombia. Ministerio de Ambiente, Vivienda y Desarrollo Territorial. Comisión Asesora Permanente para el Régimen de Construcciones Sismo Resistentes. 2017. Reglamento colombiano de construcción sismo resistente NSR-10. Asociación Colombiana de Ingeniería Sísmica.
- Harries, K, A. Sharma, B. (Eds.). 2019. Nonconventional and vernacular construction materials: Characterisation, properties and applications. Woodhead Publishing.
- ISO. "International Standard ISO 22157-1: 2019 (E), Bamboo–determination of physical and mechanical properties–Part I: Requirements. 2019.
- Deng, J., Chen, F., Wang, G. Zhang, W. (2016). Variation of parallel-to-grain compression and shearing properties in moso bamboo culm (*Phyllostachys pubescens*). *BioResources*, 11(1), 1784-1795.
- PURNOMO, M. 2001. Perilaku mekanika struktur portal bambu untuk rumah susun sederhana (Doctoral dissertation, [Yogyakarta]: Universitas Gadjah Mada).
- No, Standard. 2014 . "2800 “Iranian Code of Practice for Seismic Resistant Design of Buildings”.” forth Revision, Building and Housing Research Center, Tehran.